



---

## Wavelet Based Evaluation of Ruins of Hitit Empire

A Muhittin Albora

Istanbul University, Engineering Faculty, Geophysical Department, 34320, Avcilar, Istanbul, Turkey

**Abstract** Hittite civilisation is an historical imperial in Sivas-Kusakli during B.C. 2000 to B.C. 8000. Many geophysicians and archaeologist are still working upon the ruins of this empire. In this paper, our aim is to bring to light the archaeological structure of the North of Sivas-Kusakli using total magnetic anomalies. For this reason, wavelet and horizontal gradient-boundary analysis have been applied. The methods are also tested for synthetic examples and satisfactory results are obtained. We have extracted the historical walls which assumed to be used as towers. The circular structures closer to the considered walls are also being extracted in our studies.

**Keywords** Archaeology, Hittite Empire, Wavelet, Magnetic.

---

### Introduction

In this paper, we try to enlighten the historical Hittite civilisation which is effective in between BC second and eighth centuries. The ruins related to this civilisation are only found in Turkey which makes it interesting. The information about Labarna who is the king of Hittite Empire (BC 1650-1450) is very limited. The oldest documents belong to Labarna's son I. Hattusili (BC 1650-1620). The capital city Kussara has been removed to Hattusa (Bogazkoy) after the enlarging of the Empire toward to South of Kizilirmak. At BC 1286, the Empire has been reached to Kades placing among Yamhad and Orentes regions and has established great Hittite Empire (Fig. 1). [1, 2, 3, 4] have studied on this archaeological region.

General topographic map of Kusakli-Sarissa region is given in Figure 2. In Figure 3, the map is based on various geophysical and archeological. Afterwards, researches are focused on North side [5, 6]. In these excavations, the city walls are tried to be found by using magnetic instrumentation's. Here Fluxgate-Gradientsonden-Array, TypFoerster type magnetometer with five fluxgate-gradient drill is used. Drilling distance is 0.4 meter and the distance between the surface is about 30-40 cm. Sampling distance is about 0.1 meter (Fig. 4). Generally, wavelet has many applications on geophysics. [7] has first used the wavelet transform for potential-field data. Afterwards, [8] have worked upon seismological data. [9] had separated regional and residual potential-field anomalies using the wavelet transform. [10], processed aeromagnetic data by the wavelet transform. At the last decades, the wavelet transform has started being used in evaluation of archaeological data. [11] have used wavelet transform to magnetic synthetic examples. [12, 13] has been applied Cellular Neural Network for separation of geophysical potential field anomalies and ore areas. [14] have evaluated archaeological sites using wavelet transforms and detected the buried structures by using enhanced horizontal derivative. [15] presented modeling approach using Wavelet theory for archeological potential anomalies.

In this paper, we have applied various types of wavelet for better evaluation of total magnetic anomaly of the archaeological ruins. And also, boundary analysis is done using [16] algorithm.





Figure 1: General information about Hittite Empire

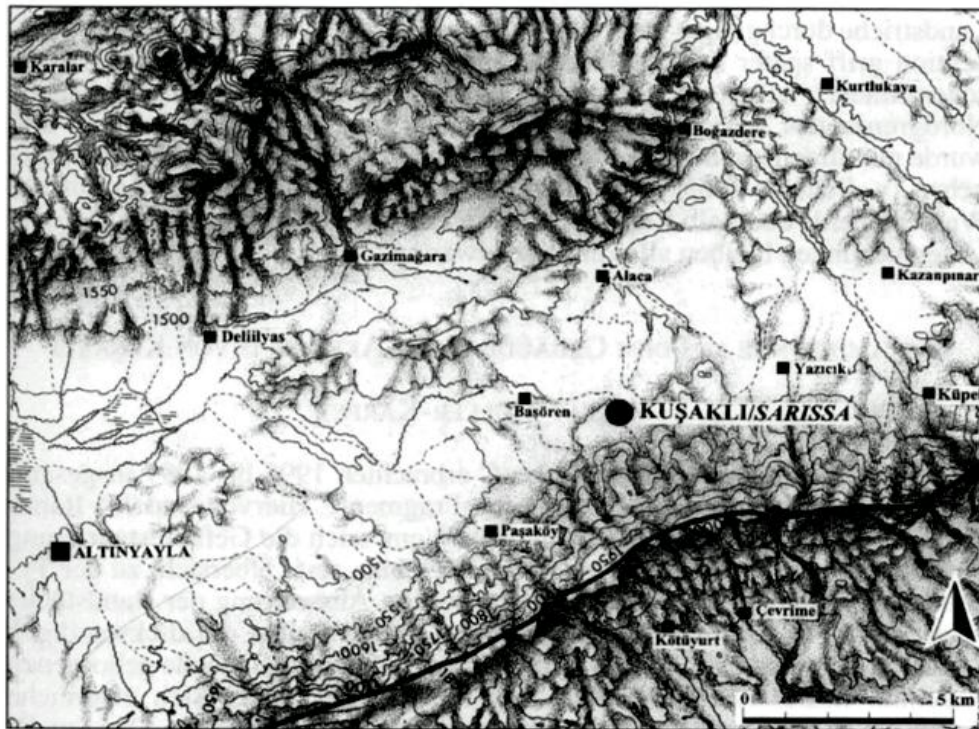


Figure 2: The ancient cities of Hittite including Kusakli-Sarissa

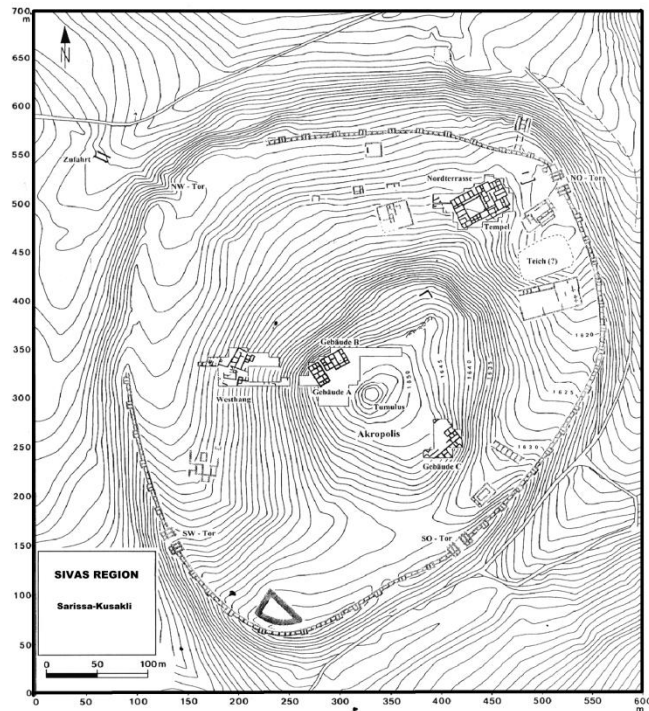


Figure 3: Topography map including excavation results.

### Applied Approaches

In this Section, wavelet and horizontal boundary analysis have been explained. Their performance is investigated for geometric prisms as synthetic examples, since our real data is the walls of Hittite Empire.

### Wavelet Transform

The wavelets, first mentioned by Haar in 1909, had compact support which means it vanishes outside of the finite interval, but Haar wavelets are not continuously differentiable. Later wavelets are considered with an effective algorithm for numerical image processing by an earlier discovered function that can vary in scale and can conserve energy when computing the functional energy [17]. In between 1960 and 1980, mathematicians such as [18] defined wavelets in the context of quantum physics. [19] gave has boosted digital signal processing by inventing the pyramidal algorithms, and orthonormal wavelet bases. [20] used Mallat's work to construct a set of wavelet orthonormal basic functions that are the cornerstone of wavelet applications today.



Figure 4: Kuşaklı-Sarissaregion using Flux-gatemagnetometers.

The class of functions that present the wavelet transform are those that are square integrable on the real time. This class is denoted as  $L^2(R)$ .

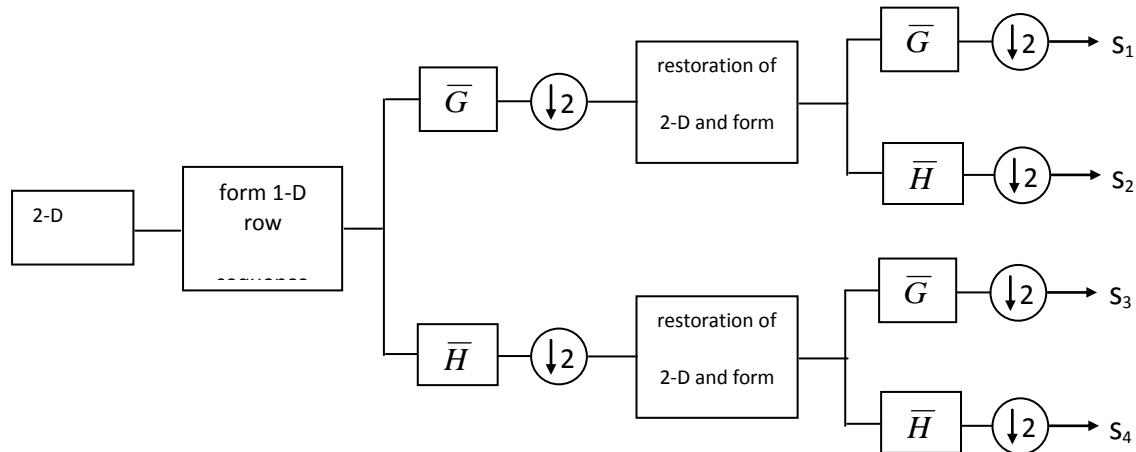


Figure 5: 2-D waveletschemewhere  $G$  is highpass,  $H$  lowpasssubbandfilteringand  $s_1, s_2, s_3, s_4$ areintermediateoutputs of wavelet.

$$f(x) \in L^2(R) \Rightarrow \int_{-\infty}^{+\infty} |f(x)|^2 dx < \infty \tag{1}$$

The set of functions that are generated in the wavelet analysis are obtained by dilating (scaling) and translating (time shifting) a single prototype function, called the mother wavelet. The wavelet function  $\psi(x) \in L^2(R)$  has two characteristic parameters, called dilation ( $a$ ) and translation ( $b$ ), which vary continuously. A set of wavelet basis function  $\psi_{a,b}(x)$  may be given,

$$\text{as } \psi_{a,b}(x) = \frac{1}{\sqrt{|a|}} \psi\left(\frac{x-b}{a}\right) a, b \in R; a \neq 0 \tag{2}$$

Here, the translation parameter, “ $b$ ”, controls the position of the wavelet in time. The “narrow” wavelet can access high frequency information, while the more dilated wavelet can access low frequency information. This means that the parameter “ $a$ ” varies for different frequencies. The continuous wavelet transform is defined by

$$W_{a,b}(f) = \langle f, \psi_{a,b} \rangle = \int_{-\infty}^{+\infty} f(x) \psi_{a,b}(x) dx . \tag{3}$$

The wavelet coefficients are given as the inner product of the function being transformed with each basis function. Daubechies (1990) invented one of the most elegant families of wavelets. They are called Compactly Supported Orthonormal Wavelets, and are used in Discrete Wavelet Transform (DWT). In this approach, the scaling function is used to compute the  $\psi$ . The scaling function  $\phi(x)$  and the corresponding wavelet  $\psi(x)$  are

$$\text{defined by } \phi(x) = \sum_{k=0}^{N-1} c_k \phi(2x - k) \tag{4}$$

$$\psi(x) = \sum_{k=0}^{N-1} (-1)^k c_k \phi(2x + k - N + 1) \tag{5}$$

where  $N$  is an even number of wavelet coefficients  $c_k, k=0$  to  $N-1$ . The discrete presentation of an orthonormal compactly supported wavelet basis of  $L^2(R)$  is formed by dilation and translation of signal function  $\psi(x)$ ,

called the wavelet function. It is assumed that the dilation parameters “a” and “b” take only the discrete values:

$$a = a_0^j, b = kb_0a_0^j, \text{ where } k, j \in Z, a_0 > 1, \text{ and } b_0 > 0.$$

Since a major potential application of wavelets is in image processing, 2-D wavelet transform is a necessity and found out as in Fig. 5.

### Application of wavelet transform to synthetic data

To test feasibility of wavelet, we have used Fig. 6. The aim of these examples is to show the performance of wavelet for detection of the prism type structures. Since our research area is generally historical walls, prism model suits well. For the archaeological data in vertical direction, we have used Fig. 6a as a representative example. In the same manner, horizontal distributed data may be found by Fig. 6a model.

The borders of the prisms are also detected on anomaly map. As it is clearly shown, the archaeological center of the buried object may not coincide with the maximum coordinates of the magnetic anomaly. The reason of this may be because of earth magnetism, the vectoral magnetism directions and object geometry. But as in Fig. 6b we can evaluate these anomalies such as gravity anomaly by using pseudo-gravity anomalies. The wavelet outputs of the input data in Fig. 6b is as in Fig. 6c. Since input data are not noisy, wavelet outputs are similar to each other. The anomalies in Fig. 6d are the horizontal components of Fig. 6c. In keen observation, it is clear that the maximum and minimum anomaly values correspond to horizontal borders of the prism. In Fig. 6e vertical component of wavelet and In Fig. 6f diagonal component of wavelet are given in Fig 6c. In this Fig. 6e maximum and minimum anomaly values give us the information about vertical borders of the prism model. In Fig. 6f diagonal wavelet outputs are shown. The maximum and minimum coordinates of the anomalies give the information about corners of the prisms.

As a result, we conclude that wavelet can denoise as in Fig. 6c and wavelet can detect the borders of an archaeological geometric structure satisfactorily by using various wavelet components.

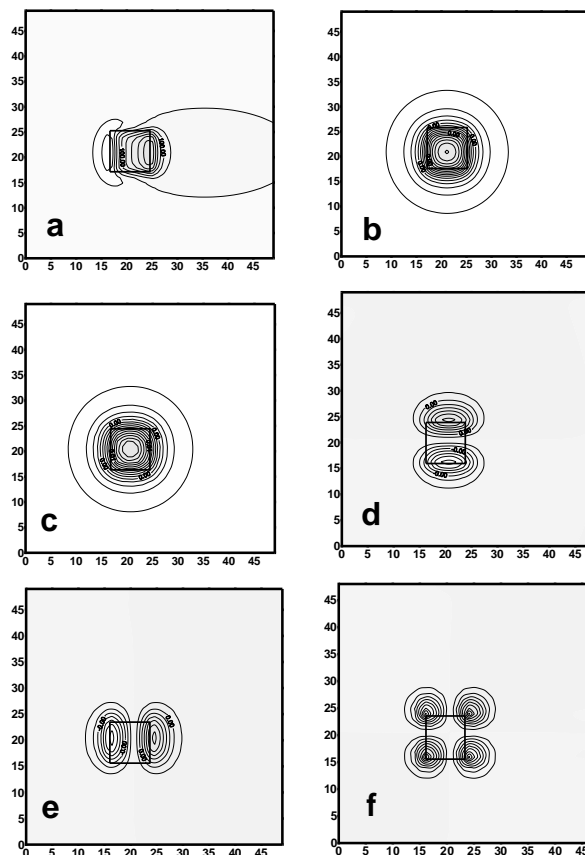


Figure 6: The vertically placed prisms model (a)- magnetic anomaly (b)- pseudo-gravity anomaly (c)- wavelet output of the pseudo-gravity anomaly (d)- horizontal component output of c (e)- vertical component output of c (f)- diagonal component output of c.

### Horizontal Gradient and Boundary Analysis

The instant variations on the density of the underground structure result instant variations in gravity anomalies. The pseudo-gravity anomaly of the magnetic anomaly is considered in similar way. The maximum coordinates of the horizontal gradient of the gravity anomaly are the borders of the geometric structure. 2-D horizontal gradient of the gravity anomaly is as,

$$h(x, y) = \left[ \left( \frac{\partial g_z(x, y)}{\partial x} \right)^2 + \left( \frac{\partial g_z(x, y)}{\partial y} \right)^2 \right]^{1/2} \quad (6)$$

The horizontal gradient of 2D gravity anomaly can easily be computed by the use simple finite-difference relations equations. Blakely and Simpson (1986) has developed this algorithm as a software program which finds out the maximum coordinates of the horizontal gradient of 2D gravity anomaly. In this study we have used third algorithm.

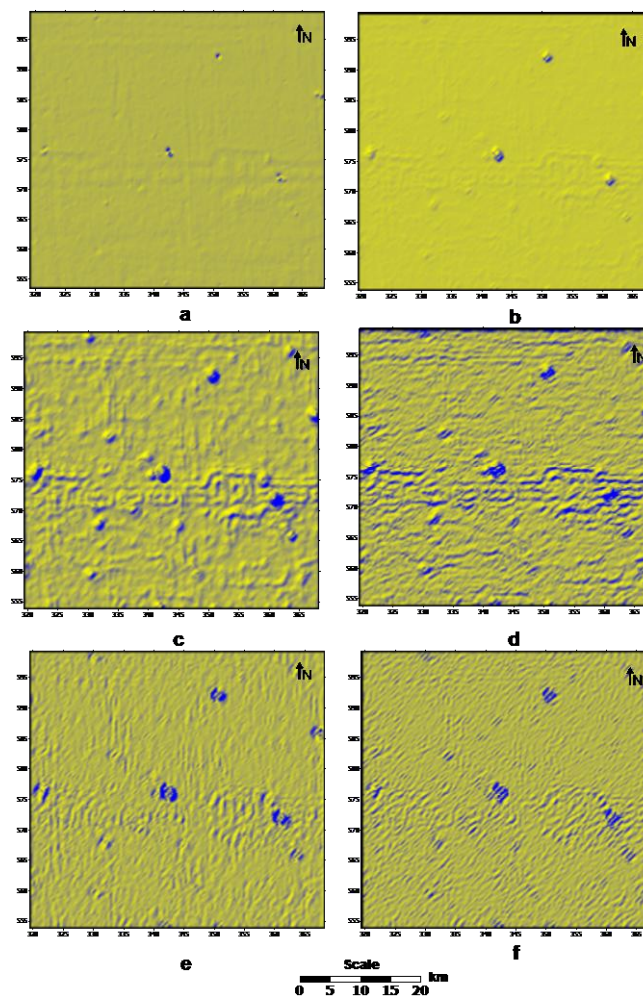


Figure 7: Sivas-Kusakli Hittite archaeological ruins (a)- magnetic anomaly (b)- pseudo-gravity anomaly (c)- wavelet output of the pseudo-gravity anomaly (d)- horizontal component output of c (e)- vertical component output of c (f)- diagonal component output of c.



## Conclusion

In previous sections, both wavelet and boundary analysis are applied to prism type synthetic examples since our real data is the historical walls with the similar geometric form of prisms. The outputs of the considered methods for Hittite Empire in Sivas-Altinyayla region are shown in Fig. 8. To evaluate the borders of the archaeological structure, we have pseudo-gravity map of the total magnetic anomaly (Fig. 8b).

The wavelet output of this pseudo-gravity map is as in Fig. 8c. At the wavelet output, horizontal, vertical directed walls and circular like structures are found out. Especially, indoor walls are clearly observed. These results can be easily shown in horizontal, vertical and diagonal components as in Fig. 8d, e and f respectively. In horizontal output, horizontal components, in vertical output, vertical components of the archaeological structure are clear. In diagonal component, circular like objects are being detected besides horizontal and vertical directed effects of the wall. Thus we can evaluate various effects of the buried objects using wavelet approach.

Thus as a result, the similar results are obtained methods. Archaeologists express that the walls are used as towers [5]. In wavelet outputs, new inner walls are found out and in both methods; new circular buried objects are detected.

Wavelet transform result of gravity anomaly in figure 8 (a) is shown. Figure 8 (b) estimated drawn by artists as a result of geophysical data images [5]. Geophysical studies depicted as estimated by archaeologists in the city of Sivas Kuşaklı as a result of the Hittite civilization.

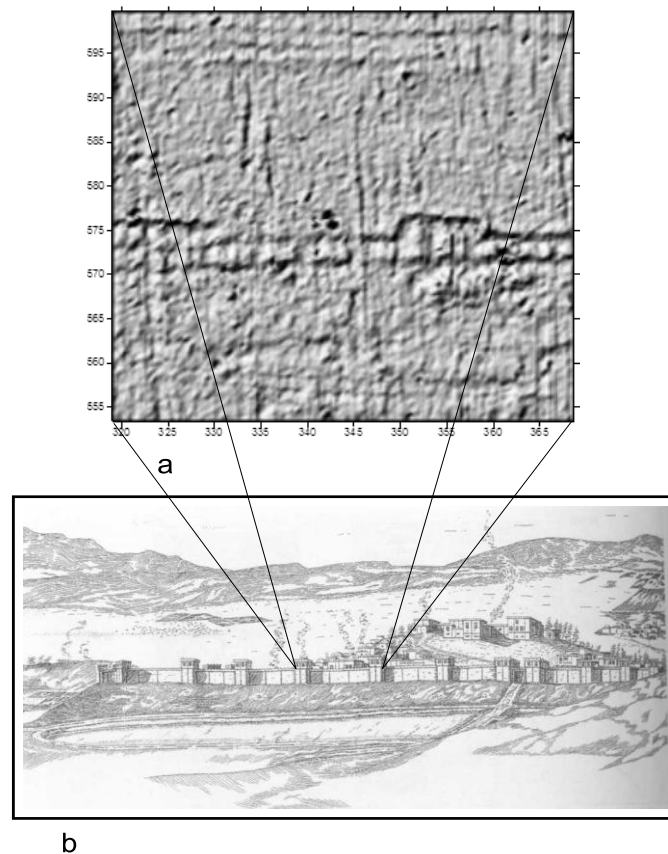


Figure 8: Sivas-Kusakli Hittite archaeological ruins (a)- wavelet output of the pseudo-gravity anomaly (b)- estimated as drawn by artist painting a result of geophysical data [5].

## Acknowledgement

This research was supported by Research Institute of Istanbul University (The Project Number: 35156). We thank Kiel and Istanbul Universities for their support of this international, inter discipline project. We also thank to Prof. Dr. Andreas Muller Karpe for their valuable comments on our paper.



**References**

- [1]. Ercan A. and Temizsöz I. (1998). Hittite Empire Period, 10x10 Squared Excavation, Geophysics and Archeological Excavation. *Turkish Geophysics* 12,35-51.
- [2]. Stumpel, H. (1996). Untersuchungen in Kusakli:GeophysikalischeProspektion, *Mitteilungen der Deutschen Orient-Gesellschaft* 128, 85-93, Berlin.
- [3]. Stumpel, H. (1997). Untersuchungen in Kusakli:GeophysikalischeProspektion, *Mitteilungen der Deutschen Orient-Gesellschaft* 129, 134-140, Berlin.
- [4]. Stumpel, H. (1998). Untersuchungen in Kusakli:GeophysikalischeProspektion, *Mitteilungen der Deutschen Orient-Gesellschaft* 130, 144-153, Berlin.
- [5]. Karpe M.A. (1998). Die hethitische StadtruineKusakli-Sarissa 1997, alma mater philippina, MarburgerUniversitätsbund 1998, 21-26.
- [6]. Karpe, M.A. (1999). 21. Excavation Results Conference Vol. 1, Cultural and Museum Ministry, 24-28 May.
- [7]. Davis A., Murshak A. and Wiscombe W. (1994). Wavelet-base multi-fractal analysis of non-stationary and/or intermittent geophysical signals. In: *Wavelets in Geophysical* (Eds E. Foufoula Georgiou and P. Kumar). 249-298. Academic Press, Inc.
- [8]. Chakraborty A. and Okaya D. (1995). Frequency-time decomposition of seismic data using the wavelet transform-based methods. *Geophysics* 60, 1906-1916.
- [9]. Fedi M. and Quata T. (1998). Wavelet Analysis for the regional-residual and local separation at potential field anomalies. *Geophysical Prospecting* 46, 507-525.
- [10]. Ridsdill-Smith, T.A. and Dentith, M. C. (1999). The wavelet transform in aeromagnetic processing. *Geophysics* 64, 1003-1013.
- [11]. Ucan, O. N., Seker, S., Albora, A. M. and Ozmen, A. (2000). Separation of Magnetic Field in Geophysical Studies Using 2-D Multi Resolution Wavelet Analysis Approach, *Journal of the Balkan Geophysical Society* 3, 53-58.
- [12]. Albora, A. M., Ucan, O. N., Ozmen, A., and Ozkan, T. (2001a), Evaluation of Sivas-Divrigi Region Akdag Iron Ore Deposits Using Cellular Neural Network, *J. Appl. Geophys.* 46, 129-142.
- [13]. Albora, A. M., Ucan, O. N., and Ozmen, A. (2001b), Residual Separation of Magnetic Fields Using a Cellular Neural Network Approach, *Pure Appl. Geophys.* 158, 1797- 1818.
- [14]. Fedi, M., and Florio, G. (2003), Decorrugation and removal of directional trends of magnetic fields by the wavelet transform: application to archaeological areas, *Geophys. Prospect.* 51, 261-272.
- [15]. Albora, A. M., Hisarlı, Z. M., and Ucan, O. N. (2004). Application of Wavelet Transform to Magnetic Data Due to Ruins of Hittite Civilization in Turkey, *Pure Appl. Geophys.* 161, 907-930.
- [16]. Blakely R.J. and Simpson R.W. 1986. Approximating edges of source bodies from aeromagnetic or gravity anomalies. *Geophysics* 51, 1494-1498.
- [17]. Gabor D. (1946). *Theory of Communications* J. IEEE, 93, 3, 429.
- [18]. Grossman A., Morlet J. (1985). *Mathematics and Physics 2*, (Ed. L. Streit) World Scientific Publishing, Singapore.
- [19]. Mallat, S. (1989). A Theory for Multi-resolution Signal Decomposition the Wavelet Representation, *IEEE Trans. Pattern Anal. And Machine Intelligence* 31, 679-693.
- [20]. Daubechies I. (1990). The Wavelet Transform, Time-Frequency Localization and Signal Analysis, *IEEE Trans, On Information Theory*, 36.

